Characterization of char generated from solar pyrolysis of heavy metal contaminated biomass

Kuo Zeng, Rui Li, Doan Pham Minh, Elsa Weiss-Hortala, Ange Nzihou, Dian Zhong, Gilles Flamant

Energy 206 (2020) 118128

Contents lists available at ScienceDirect

Energy

journal homepage: www.elsevier.com/locate/energy

Characterization of char generated from solar pyrolysis of heavy metal contaminated biomass

Kuo Zeng [a, c], Rui Li [a], Doan Pham Minh [b], Elsa Weiss-Hortala [b], Ange Nzihou [b], Dian Zhong [c], Gilles Flamant [a, *]

[a] Processes, Materials and Solar Energy Laboratory, PROMES-CNRS, 7 Rue du Four Solaire, 66120, Odeillo Font Romeu, France
[b] Université de Toulouse, IMT Mines Albi, UMR CNRS 5302, Centre RAPSODEE, Campus Jarlard, F-81013, Albi Cedex 09, France
[c] State Key Laboratory of Coal Combustion, Huazhong University of Science and Technology, 1037 Luoyu Road, Wuhan, Hubei, 430074, PR China

ARTICLE INFO

Article history:
Received 5 April 2020
Received in revised form
25 May 2020
Accepted 11 June 2020
Available online 17 June 2020

Keywords:
Solar pyrolysis
Willow
Heavy metals
Char characterization

ABSTRACT

Solar pyrolysis of raw and heavy metals (HMs) impregnated willow was performed at different temperatures (600, 800, 1000, 1200, 1400 and 1600 °C) with heating rate of 50 °C/s. CHNS, ICP-OES, SEM-EDX and BET were employed to investigate the effects of temperature and HMs contamination on char properties. The results indicated that a more ordered and aromatic char was formed with increasing pyrolysis temperature. Char carbon contents increased from 70.0% to 88.4% while hydrogen and oxygen contents declined. Char BET surface area firstly increased from 5.3 to 161.0 m^2/g with rising the temperature from 600 to 1000 °C, then decreased at higher temperatures due to plastic deformation. Pyrolysis caused alkali and alkaline-earth metals (A&AEMs) enrichment in char as temperature increased from 600 to 800 °C, then their content decreased at higher temperatures. The presence of Cu or Ni led to the decrease of hydrogen and oxygen contents and significant increase of Ni or Cu in char compared with those in raw willow char. Besides, Raman and BET analysis showed that contaminated willow char had a higher ratio of G band area to the integrated area (I_G/I_{All}) and bigger BET surface area than raw material indicating a more organized and porous structure of the char.

1. Introduction

A lot of soil and water are contaminated by heavy metals, which is a serious environmental problem in the world. HMs extraction by plants called phytoextraction has been viewed as an environmentally effective option for large area contamination abatement [1]. Such kind of plants called hyperaccumulators can absorb HMs with roots and accumulate them in tissues and structures [2]. Willow that is a kind of fast growing hyperaccumulator has been widely used for agricultural soil remediation. For example, the contents of copper and nickel in phytoextraction willow are hundreds to thousands times higher than those in polluted soil [3]. To prevent metal dissemination again, the HMs contaminated biomass have to be disposed off in a safe way [4].

Pyrolysis is proposed as a feasible, economical and environmentally post-treatment method, which can recycle HMs contaminated biomass into valuable products (gas, oil and char) [5]. HMs contaminated biomass volume is reduced a lot with minimized pollution discharge [6]. The treatment cost through pyrolysis according to economic evaluation is far less than that through conventional way like leaching [7]. Pyrolysis aims to concentrate HMs in the char and utilize valuable by-products (oil and gas) without secondary heavy metal pollution [8]. Koppolu et al. investigated the pyrolysis of HMs (Ni, Zn, Cu, Co, or Cr) polluted biomass at 600 °C in a fluidized bed reactor and found that more than 98.5% of HMs was retained in the char, whose metal concentration ranged from 0.7 to 15.3% [9–11]. Solar pyrolysis enables high temperature and fast heating rate, therefore it satisfies the requirement of treating HM contaminated biomass [12]. Besides, low heating value (LHV) of pyrolysis products is higher than LHV of initial biomass since pyrolysis reaction is driven by concentrated solar radiation without combustion of part of the biomass [13–15]. Therefore, solar pyrolysis of heavy metal contaminated biomass at temperatures from 600 to 1600 °C with heating rate of 50 °C/s for gas fuel production has been carried out [6]. However, HMs loaded char properties should be determined before further utilization.

Temperature is the main factor affecting the chemical, structure

* Corresponding author.
E-mail address: gilles.flamant@promes.cnrs.fr (G. Flamant).

https://doi.org/10.1016/j.energy.2020.118128

and morphology transformation of pyrolysis char [8,16]. The carbon content in char increases with pyrolysis temperature as well as structure order [2]. The hydrogen and oxygen contents in char decrease at the same time [17]. Furthermore, Raman spectrum ratio ID/IG of beech wood char increases from 0.76 to 1.2 with the pyrolysis temperature rising from 500 °C to 1400 °C due to condensed aromatic structure formation from small structures [18]. The char BET surface area exhibits a maximum with temperature. It firstly increases with temperature due to the intensified volatile release [19]. However, the char underwent plastic deformation with micropores collapse when temperature rises above 1000 °C, which causes BET surface area decrease [18,20]. Temperature also influences minerals (HMs and A&AEMs) distribution in pyrolysis products [2]. At mild temperatures (300–400 °C), organic compounds decomposition is stronger than minerals' evaporation resulting in mineral enrichment in char [21]. With pyrolysis temperature increasing above minerals' boiling point, their evaporation becomes stronger than organic compounds decomposition, which results in the decrease of minerals concentration in char [22]. Davidsson et al. found that A&AEMs (Ca, Mg, K and Na) are released from wood during pyrolysis at 250–400 °C and are further emitted from char ash fraction at temperatures above 600 °C [23]. The first release stage is due to the decomposition of organic metal salts in the range 300–400 °C, while the second emission is attributed to inorganic metal compounds evaporation [24].

HMs such as Cu and Ni could act as in-situ catalysts on contaminated biomass pyrolysis reactions, which may affect the char product properties [25]. Copper effectively catalyzes the chain-breaking of lignin at 450–600 °C that can promote to some extent the C and H cleavage from solid matrix [7]. Similarly, Nickel catalyzes carboxyl and carbonyl bond breaking from biomass for more CO_2 formation, which results in the decrease the C and O contents in char [26]. Ni or Cu impregnation in wood samples does not lead to major changes in the behavior of other minerals like A&AEMs [3]. However, Ni or Cu contents in char from impregnated biomass pyrolysis might increase significantly compared with those in raw willow pyrolysis char due to Cu or Ni embedded into carbon matrix. For example, Ni content in Ni-impregnated rice husk pyrolysis char was 49.58%, much higher than that in raw rice husk pyrolysis char (0.22%) [26]. After pyrolysis at temperature of 350, 550 and 750 °C, the Cu contents in char obtained from Cu polluted biomass were 16.29, 19.24 and 22.11 mg/g, which were much higher than those of 1.03, 0.12 and 0.02 mg/g in char from raw biomass, respectively [19].

Properties of chars derived from contaminated biomass pyrolysis under different conditions have been reported. However, properties of char generated from solar pyrolysis of heavy metal contaminated biomass under high temperature and heating rate has not yet been reported. After understanding how solar pyrolysis conditions (temperature) and feedstock characteristics (HM content) affect chemical, structure and morphology transformation of char, one can more readily process char into desired forms for further valuable use. In this study, solar pyrolysis of raw and heavy metal (HM) impregnated willow was performed under different temperatures (600, 800, 1000, 1200, 1400 and 1600 °C) with a heating rate of 50 C/s. CHNS analysis, Raman spectroscopy, BET and ICP-OES measurements and SEM-EDX observations were employed to investigate the effects of temperature and HMs contamination on pyrolysis char properties.

2. Experimental

2.1. Sample preparation

Raw and Cu and Ni impregnated willow samples were prepared. 100 g willow wood particles were impregnated with 1 L of $Ni(NO_3)_2 \cdot 6H_2O$ or $Cu(NO_3)_2 \cdot 6H_2O$ (Sigma-Aldrich, 99% purity). After stirring of the mixture at ambient temperature for 24 h, the impregnated willow wood was filtered and dried at 60 °C for 24 h. Then, the raw and the impregnated willow wood were compressed into pellets. The pellets with 10 mm in diameter and 5 mm in height corresponding to about 0.3 g were used in the experiments. The raw willow wood, Cu contaminated willow wood and Ni contaminated willow wood characteristics measured by CHNS and ICP-OES are shown in Table 1.

2.2. Solar pyrolysis experiment

2.2.1. Experimental setup

A vertical axis solar furnace was used to perform the solar pyrolysis experiments with the same experimental setup as in our previous study, it is shown in Fig. 1 [6]. The solar furnace power and flux density were about 1.5 kW and 12,000 kW/m^2, respectively. A graphite crucible was set at the focus of solar furnace holding the biomass pellet. The solar reactor was composed of two main parts, a metallic vessel and a transparent Pyrex window. The reactor was swept with an argon flow controlled by a mass flowmeter. A water-cooled sample holder was assembled with the metallic vessel. This sample holder moved in and out of the vessel to insert and extract the sample pellet. The window was equipped with a porthole to measure the pellet temperature with a solar-blind optical pyrometer. A shutter controlled the temperature and heating rate of the pellet during pyrolysis. The shutter associated with a PID controller was located between the heliostat and the parabola. With such a high heat flux, high heating rate and temperature can be easily reached with high speed opening of the shutter. The degree and speed of the shutter opening were controlled to fit the chosen final temperature and heating rate.

2.2.2. Experimental procedure

The reactor was swept by argon gas three times separated by a pumping step. Then, the target temperature and heating rate was set on the PID controller. The shutter was open accordingly and the pyrolysis started. The solid residue resulting from solar pyrolysis regarded as char was cooled to the room temperature inside the crucible. The char was weighed for determining the yield and then stored in a desiccator for subsequent analyses. Pyrolysis was performed for six different temperatures (600, 800, 1000, 1200, 1400 and 1600 °C) with the heating rate of 50 °C/s under Argon (9 NL/min flow rate). The duration of plateau temperature was 5 min. Each

Table 1
Element concentrations in biomass feedstock.

Sample	%				Total element concentrations (mg/kg)						
	C	H	O	N	Ca	K	Mg	Na	Si	Cu	Ni
Raw willow	48.8	5.9	43.8	0.6	4255	847	275	168	218	25	3
Willow+Ni	48.7	5.8	43.9	0.7	4172	699	174	149	157	22	5632
Willow+Cu	48.6	6.0	44	0.6	4125	764	163	135	142	5156	3

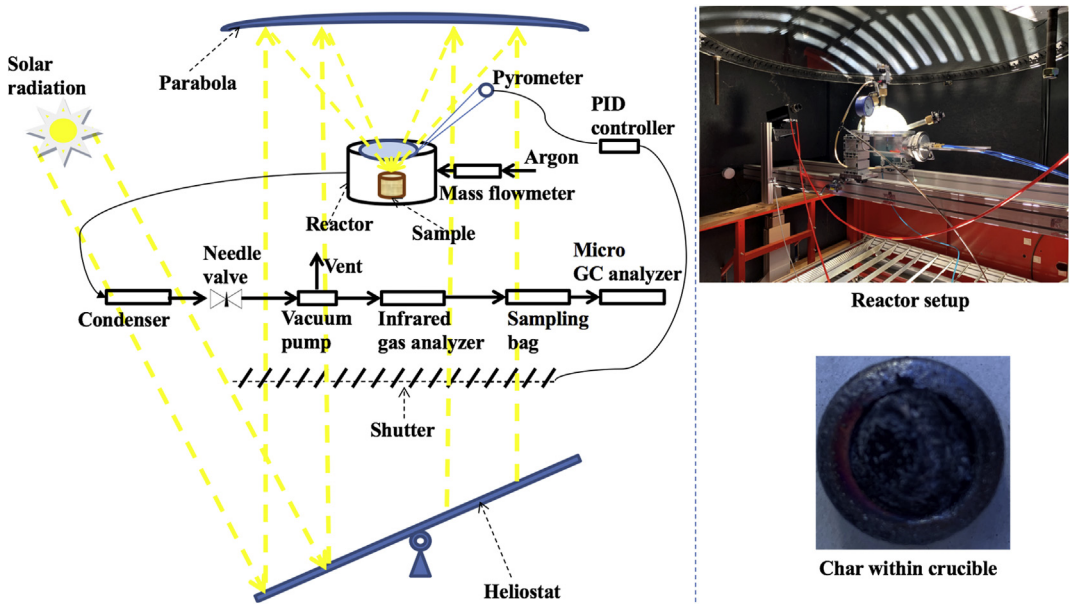

Fig. 1. Schematic of solar pyrolysis experimental setup.

treatment was triplicated and the repeatability was satisfying, the difference between test data was always less than 5%.

2.2.3. Sample characterization

The elemental compositions (C, H, N, S) of the samples (raw willow, impregnated willow, raw willow char and impregnate willow char) were determined with an elemental analyzer (Flash 2000). The oxygen content was determined by mass balance. Besides, all samples were mineralized with a specific mineralization protocol described by Said et al. [3], which then analyzed by inductively coupled plasma optical emission spectroscopy (ICP-OES, HORIBA Jobin Yvon ULTIMA-2) for determination of inorganics. Additionally, scanning electron microscopy (SEM) together with an energy dispersive X-ray analyzer (SEM-EDX, Hitachi S4800, Japan) was used to investigate the microstructure and elemental distribution on char samples. In order to prepare specimens for SEM-EDX analysis, char samples were coated with a 2–3 nm Au/Pd layer to ensure electrical conductivity. Raman spectroscopy (Confocal Raman-AFM WITEC Alpha 300AR microscope equipped with a CCD camera detector) was used to determine the carbon structure of the chars at the particle surface (on a square of 5 μm). Spectra were recorded using a lens 50 and an excitation laser at 532 nm in the region of 175–4000 cm^{-1} of Raman shift. The surface area of char was measured by N_2 adsorption with the Brunauer- Emmett- Teller method (BET Tristar II 3020 Micromeritics).

3. Results and discussion

3.1. Char composition

Char yields obtained from solar pyrolysis of heavy metal contaminated willow at different pyrolysis temperatures have already been indicated in our previous study. It varied from 27, 24 and 22% to about 10% for raw, Cu-impregnated and Ni-impregnated willow respectively for a temperature increasing from 600 °C to 1600 °C [6]. Fig. 2 presents the elemental composition of the chars from raw and impregnated willow under different pyrolysis temperatures. Whatever the type of pyrolysis feedstock, the carbon mainly remains in char. This means that it becomes more aromatic [16]. For raw willow pyrolysis (Fig. 2a), carbon content increases from 70.0% to 88.4%, while the hydrogen and oxygen contents sharply decreases from 3.6% to 0.4% and 25.7%–11.2%, respectively with temperature increasing from 600 to 1600 °C. For impregnated willow pyrolysis, the carbon contents also increase with declining hydrogen and oxygen contents. As shown in Fig. 2b, carbon content increases from 71.0% to 87.7%, while the hydrogen and oxygen contents decrease from 3.3% to 0.2% and 25.0%–10.2% for Cu contaminated willow pyrolysis char, respectively. These results are consistent with the chemical composition of solar pyrolysis char explained by enhanced breaking of weak chemical bonds with increasing temperatures [15,17].

The presence of heavy metals (Cu or Ni) leads to a significant decrease of char hydrogen and oxygen contents compared with raw willow char. In the temperature range from 600 to 1600 °C, hydrogen and oxygen contents of nickel impregnated willow pyrolysis char decrease from 2.6% to 0.2% and 24.5%–10.0%, respectively (compared to a decrease from 3.6% to 0.4% and 25.7%–11.2% for raw willow) (Fig. 2c). It is assumed that copper or nickel could promotes depolymerization of cellulose and hemicellulose especially C–H and C–O bonds cleavage [25]. Besides, copper and nickel have noticeable catalytic activity with respect to tar cracking and reforming into H_2 and CO, which could further decrease hydrogen and oxygen contents in char [3].

3.2. Char morphology and structure

3.2.1. Raman analysis

Initial data were fitted into Lorentzian profile, for the G (1580 cm^{-1}), D1 (1350 cm^{-1}), D2 (1620 cm^{-1}) and D4 (1150 cm^{-1}) bands and Gaussian profile for the D3 (1530 cm^{-1}) band [27]. G band was used to study graphitic lattice, as an indicator of the char graphitic order. D1 and D2 bands were originated from disordered graphitic lattices vibration mode. D3 and D4 bands were attributed to the amorphous carbon and mixed sp2-sp3 bonds, respectively [28]. The band area ratios, including those of the defect bands to the G band (denoted as I_{D1}/I_G, I_{D2}/I_G, I_{D3}/I_G and I_{D4}/I_G) and that of the G band relative to the integrated area under the spectrum (denoted as

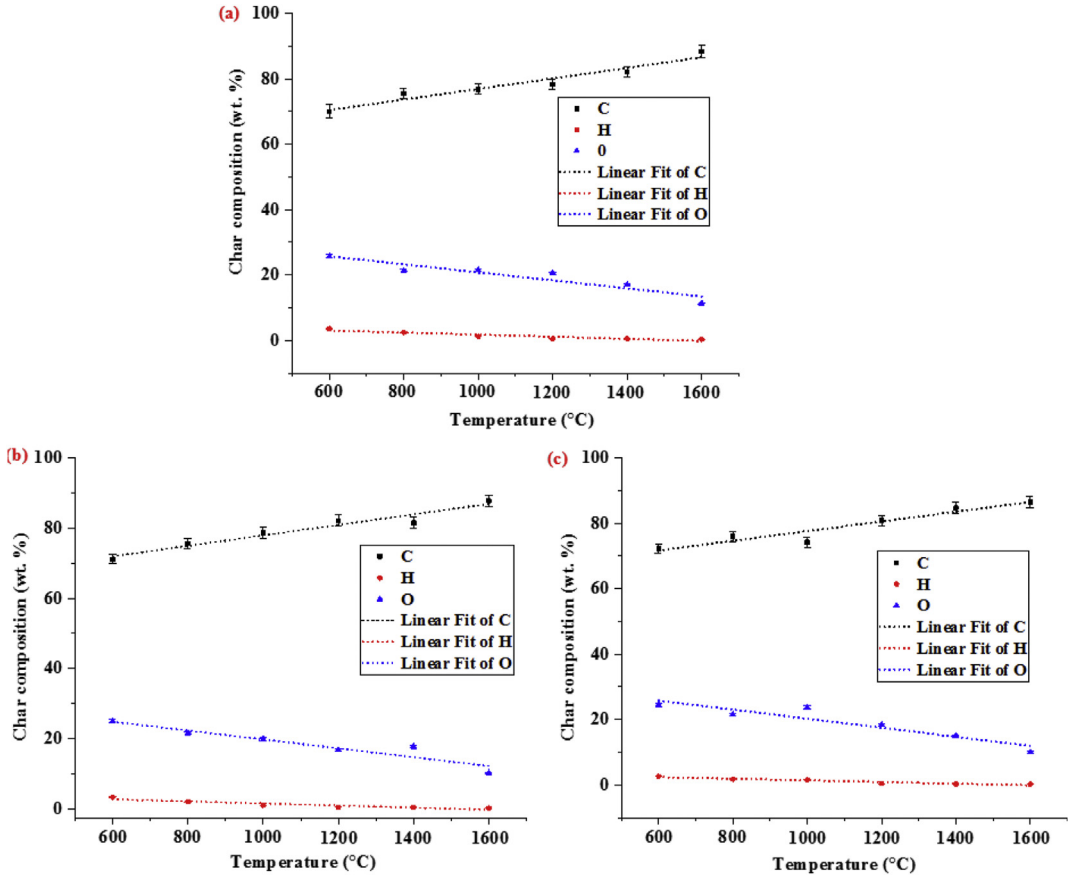

Fig. 2. Effects of temperature and HMs contamination on solar pyrolysis char composition: (a) raw willow, (b) willow with Cu, and (c) willow with Ni.

I_G/I_{All}) for all chars are shown in Fig. 3.

The ratios I_{D1}/I_G, I_{D2}/I_G and I_G/I_{All} correspond to microcrystalline planar size, graphitic domains thickness and graphitic lattice proportion, respectively [29]. Fig. 3 indicates that I_{D1}/I_G, I_{D2}/I_G, I_{D3}/I_G and I_{D4}/I_G band ratios decrease with the increase of the pyrolysis temperature for all chars, while I_G/I_{All} increases. The downward trend of band area ratios indicates that various forms of structural and carbon crystallites defects are gradually eliminated when undergoing a severe heat treatment [30]. It is generally accepted that the correlation between the ratio I_{D1}/I_G and the crystallite size shows an inverse proportional behavior [18]. Therefore, the decrease in I_{D1}/I_G means an increase in the average planar size of the graphite microcrystals. In addition, the decrease in I_{D3}/I_G and I_{D4}/I_G indicates that the amorphous phase of char is converted into a crystalline form. As a result, a more organized char structure is formed as the temperature increased, which led to an increase in I_G/I_{All}.

For impregnated willow pyrolysis chars (Fig. 3b and c), a similar trend of the band area ratios as a function of temperature is observed. Generally, Cu chars and Ni chars are found to have a higher I_G/I_{All} ratio and lower I_{D1}/I_G, I_{D2}/I_G, I_{D3}/I_G and I_{D4}/I_G ratios than raw willow implying to be more ordered and aromatic than raw chars generated at the same temperature in the range 1000–1600 °C. Guizani et al. developed a correlation between both ratios ID/IG and (O+H)/C, which proved that char ordering was highly correlated to H and O departure into the gas phase [18]. Besides, the presence of heavy metals (Cu or Ni) during willow pyrolysis increases large aromatic rings proportion as indicated by the lower I_{D1}/I_G ratio compared to raw willow. Tay et al. found that the presence of minerals favored the formation of large aromatic rings systems in reducing atmosphere [31]. I_{D3}/I_G and I_{D4}/I_G were treated as indicators for char active sites [29]. Chars derived from metal-impregnated willow pyrolysis exhibit a lower $I_{(D3+D4)}/I_G$ than raw willow char, which denotes a lower reactivity. It is mainly due to amorphous carbon and mixed sp2-sp3 bonds disappearing with the catalytic effect of Cu and Ni during pyrolysis.

3.2.2. BET analysis

Table 2 shows the effects of temperature and HMs contamination on BET surface area. For both chars generated from raw willow and impregnated willow, BET surface area exhibits a maximum at about 1000 °C in the temperature range 600–1600 °C. These results are in agreement with the literature data showing that rice straw pyrolysis char total surface area firstly increased with temperature up to 900 °C and then decreased at higher temperatures [32]. The increase could be attributed to the intensifying volatile release during pyrolysis, resulting in the formation of internal porous structure [19]. However, thermal deactivation of char might dominate during pyrolysis over 900 °C, which induced pore fuse, structure ordering and char melting [33].

The BET surface area of raw willow char (161 m^2/g) obtained at 1000 °C is drastically lower than that of Cu contaminated willow char (320 m^2/g) and Ni contaminated willow char (359 m^2/g), implying that the presence of heavy metal leads to a sharp increase in the BET surface area. The presence of heavy metals (Cu and Ni) promotes C–H and C–O bonds cleavage from char with enhancing gas release, which favors micropore formation [34]. However, there is almost no difference of BET surface area for chars of raw willow and contaminated willow at 600 °C. This result agrees with the literature data explaining that, at this temperature, some

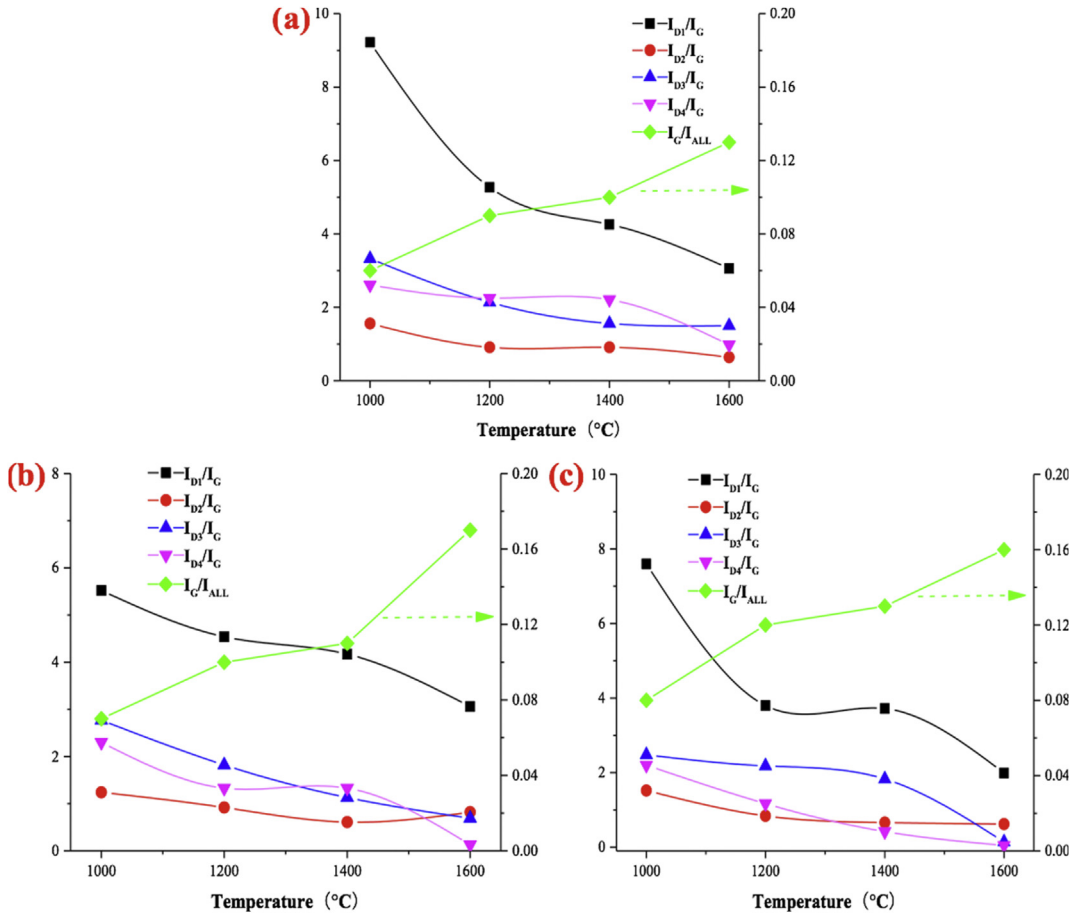

Fig. 3. Effects of temperature and HMs contamination on Raman band area ratios of solar pyrolysis char: (a) raw willow, (b) willow with Cu, and (c) willow with Ni.

Table 2
Effects of temperature and HMs contamination on solar pyrolysis char BET surface area.

Char samples	BET surface area (m^2/g)
Raw-600 °C	5.3
Raw-1000 °C	161.0
Raw-1600 °C	21.2
Cu-600 °C	7.8
Cu-1000 °C	320.0
Cu-1600 °C	41.5
Ni-600 °C	10.2
Ni-1000 °C	359.0
Ni-1600 °C	60.2

micropores are blocked by heavy metal nanoparticles even considering their catalytic effect on gas formation [26,35].

3.3. Char mineral composition

3.3.1. ICP-OES

ICP-OES analysis was carried out for chars prepared with raw willow and contaminated willow at different pyrolysis temperatures. ICP measurement was repeated three times. All relative standard deviations were less than 0.6%. The mineral elements shown in Fig. 4 are mainly categorized into A&AEMs elements (Ca, K, Mg, Na), Si and heavy metal elements (Cu, Ni) according to their abundant order. As can be seen, A&AEMs elements in raw willow chars are majority, their amounts are about 300 times larger than heavy metal elements. The Cu or Ni contents in char obtained from

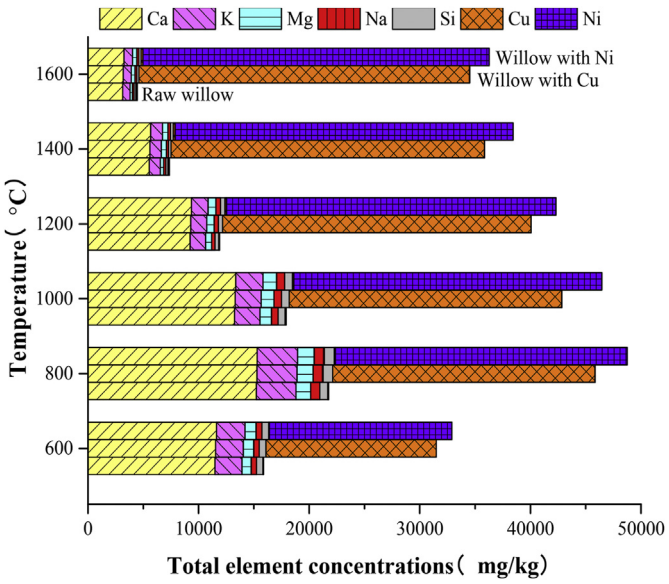

Fig. 4. Effects of temperature and HMs contamination on solar pyrolysis char mineral element concentration.

HMs contaminated willow was much higher than those in willow feedstock. It agreed well with the results of Liu et al. [7]. In addition, heavy metal element concentrations are very low indicating no risk [36]. As temperature increased from 600 to 800 °C, pyrolysis caused

A&AEMs elements enrichment in the char. For instance, the concentration of Ca and K increase from 11,473 to 2457 mg/kg at 600 °C to 15,230 and 3573 mg/kg at 800 °C. This finding agrees well with other similar study [37]. This trend could be due to the combined effect of two processes: organic compounds decomposition for volatile release and inorganic elements evaporation [21]. The first process causes strong C, H and O elements loss in solid matrix contributing to the increase of mineral elements relative content. The second process induces volatilization of mineral elements. Organic compound decomposition seems to be dominant over

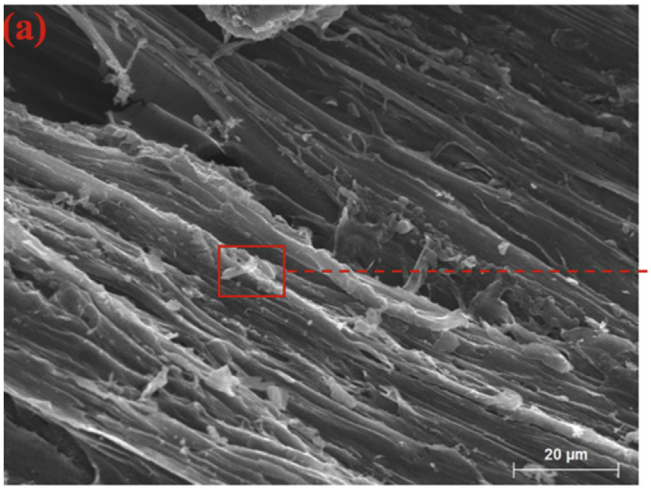

Elem	wt. %
C	70.5
O	13.7
Ca	14.7
Cu	0.8
Ni	0.3

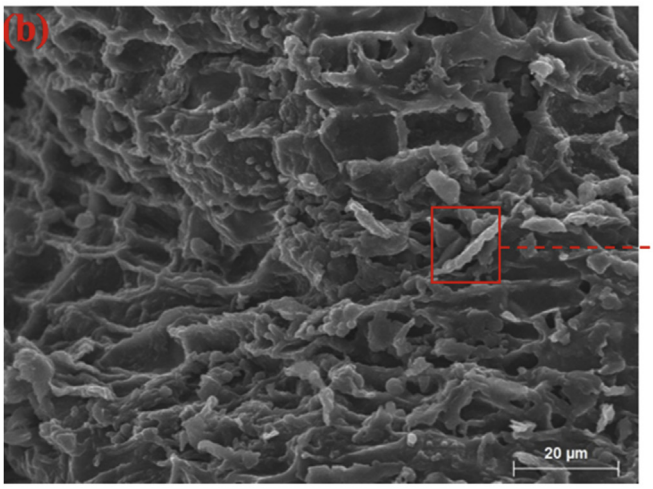

Elem	wt. %
C	74.5
O	7.2
Ca	9.2
Si	3.2
K	4.2
Cu	1.1
Ni	0.6

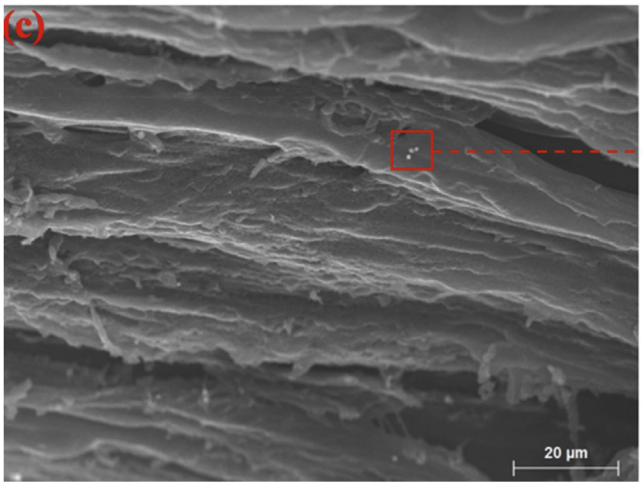

Elem	wt. %
C	87.5
O	1.5
Ca	4.2
K	1.0
Cu	4.1
Ni	1.7

Fig. 5. SEM-EDX analysis of solar pyrolysis raw willow char: (a) 600 °C, (b) 1000 °C, and (c) 1600 °C.

mineral elements evaporation as their volatilization rates are small at this temperature range.

Contrarily, A&AEMs elements contents decrease in the char with pyrolysis temperature further increasing from 800 to 1600 °C. This result is consistent with the change of dominant process, metal vaporization becoming more and more intense with the temperature increase [38]. In contrast, pyrolysis temperature from 600 to 1600 °C has no influence on the volatilization of Cu and Ni [39]. As a result, the Cu and Ni element contents increase in all of the char due to the enhanced organic compound decomposition. Besides, there is a small increase of A&AEMs elements content in the char from willow wood impregnated with Cu or Ni compared to those of raw willow char. This trend is assumed to be linked to the catalytic effects of Cu or Ni for promoting C—H and C—O bonds cleavage from char [38].

3.3.2. SEM-EDX

Fig. 5 presents SEM images of raw willow char prepared at 600 °C, 1000 °C and 1600 °C with EDX analysis of selected areas. As shown in Figs. 5a and 600 °C raw willow char contains mainly large fibrous texture nodules with some spherical shape and cavities. Char chemical composition is not uniform at micro-scale [16]. One white cubic grain can be clearly seen in the Fig. 5a, as indicated by rectangle with an arrow. From this grain, high content of Ca with some carbon and oxygen were detected by EDX analysis. Besides, traces of Cu and Ni were also detected. One can assume that calcium carbonate was initially at this location and not moving on the surface. It was not possible to confirm the diffusion of minerals from the core to the surface at this stage. HMs were mainly enriched in char at low pyrolysis temperature, while there was only trace amount release to gas and oil products [40]. Syc et al. found that HMs vaporization increases in the subsequent order: Ni, Cu, Zn, Pb, Cd, among them Ni and Cu have a very low volatility even at temperature of 850 °C [41]. Equilibrium calculations also predict no significant volatilization of Ni and Cu at 850 °C [42].

As the pyrolysis temperature increases to 1000 °C, more twisted and rough char is formed with some pore collapse indicated in Fig. 5b. It is due to the intensified volatile release with the temperature increase resulting in more cracks and pores formation [43]. It indicates that increasing pyrolysis temperature to a certain extent benefits the char porosity increase as proved by previous BET analysis [19]. However, char partial melting is observed as indicated by the rectangle, at this location high concentrations of Si, K and Ca are detected by EDX analysis. During pyrolysis at 1000 °C, K vaporizes and migrates from biomass matrix to its surface. Potassium silicates might form when K vapor contacts with silica, whose melting temperature was about 600 °C [44]. The widely distributed A&AEMs elements like Ca as oxides in biomass tend to react with molten potassium silicates to form K—Ca-silicates delaying their release [20]. Ca and Mg are more inclined to be retained in char than Na and K [45]. Besides, alkaline elements amount in 1000 °C char grains reduce compared with those in 600 °C char. It indicates more intensive alkaline elements vaporization at higher temperature than 1000 °C. Increasing pyrolysis

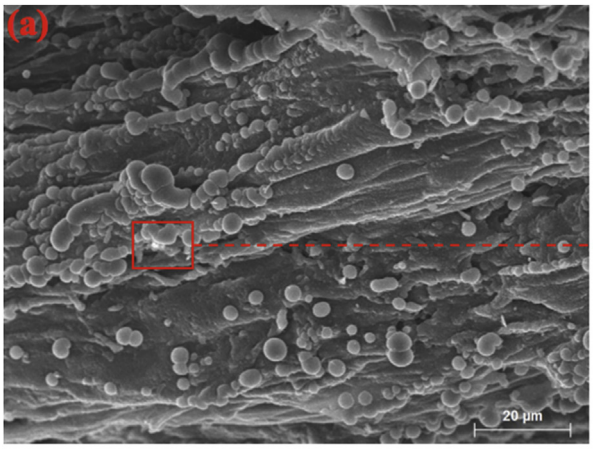

Elem	wt. %
C	78.5
O	1.8
Ca	2.2
Cu	15.6
Ni	1.9

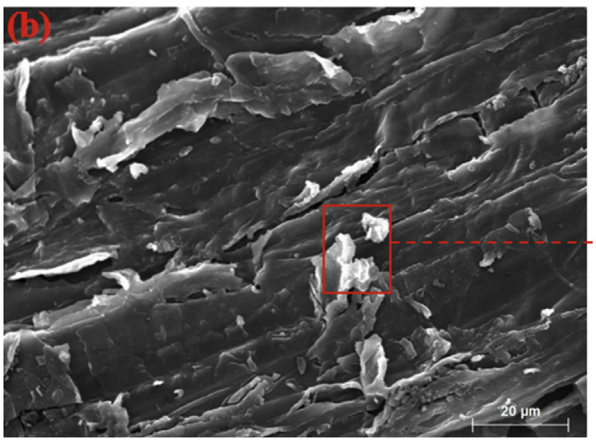

Elem	wt. %
C	80.2
O	1.1
Ca	1.7
Cu	2.7
Ni	14.3

Fig. 6. SEM-EDX analysis of solar pyrolysis HM contaminated willow char at 1600 °C: (a) With Cu and (b) with Ni.

temperature promotes A&AEMs species vaporization, mainly M_XCO3 and M_XO, leaving cavities on char surfaces [44]. Although, HMs release to the gaseous phase gradually increased with temperature due to the metal compound vapor pressure increase enhancing their diffusion rates [46]. The Cu or Ni content in char still increased as pyrolysis temperature increased from 600 to 1000 °C. It is in accordance with that the concentration of Cu and Ni in char increased from 30.25 to 62.74 μg/g and 1.68–3.17 μg/g, respectively with pyrolysis temperature increasing from 300 to 800 °C [21].

When pyrolysis temperature increases to 1600 °C, the char experiences plastic deformation as shown in Fig. 5c. A smooth and compact structure of char surface is developed due to sintering effect, in agreement with our previous study [17]. At severe devolatilization condition like high temperature, char plastic transformation may occur due to solid matrix softening and cell structure melting, which leads to pore closing [47]. EDX analyses of small grains on char surfaces reveal that most of A&AEMs elements migrate and coalesce during vaporization. Meanwhile, small part of A&AEMs is retained and stays incorporated into char matrix. The 1600 °C char particles have significantly higher content of Cu and Ni in the small grains on char surface than those of 600 and 1000 °C char because almost no volatilization of Cu and Ni occurs [39].

The changing trend of char morphology with temperature was almost the same for raw willow and heavy metal impregnated willow. SEM images with corresponding EDX of chars prepared with Cu impregnated willow and Ni impregnated willow at 1600 °C are presented in Fig. 6. There are few A&AEMs on char surface grains, such as Ca. While the Cu content in Cu impregnated willow char (Fig. 6a) and Ni content in Ni impregnated willow char (Fig. 6b) increase significantly compared to raw willow char, indicating that the impregnated Cu or Ni has been embedded into carbon matrix. According to EDX, the Cu content in Cu-char grain and Ni content in Ni-char grain increase to 15.6% and 14.3%, respectively. These results are in agreement with literature about Fe and Ni enrichment in their impregnated rice husk pyrolysis char [26].

4. Conclusion

Solar pyrolysis temperature and heavy metal affected the char properties. A more ordered and aromatic char was formed with increasing pyrolysis temperature, which carbon content increased while hydrogen and oxygen content declined. Char BET surface area exhibited a maximum at approximately 1000 °C, the decreased at higher temperature was due to plastic deformation. Besides, the BET surface area of raw willow char (161 m^2/g) obtained at 1000 °C was lower than that of Cu contaminated willow char (320 m^2/g) and Ni contaminated willow char (359 m^2/g). Pyrolysis caused alkaline elements enrichment in the char as temperature increased from 600 to 800 °C. At higher temperature, alkaline content decreased due to enhanced vaporization. The addition of Cu or Ni led to the decrease of hydrogen and oxygen contents. Contrarily, the significant increase of Ni or Cu in char with temperature indicated that the vaporization of both metals was small by comparison with alkaline elements. Copper and nickel contaminated willow pyrolysis chars were found more organized by comparison with raw willow char as proved by Raman spectra showing a higher I_G/I_{All} ratio and lower I_{D1}/I_G, I_{D2}/I_G, I_{D3}/I_G ratios.

CRediT authorship contribution statement

Kuo Zeng: Formal analysis, Writing - original draft. **Rui Li:** Data curation. **Doan Pham Minh:** Data curation. **Elsa Weiss-Hortala:** Data curation. **Ange Nzihou:** Supervision, Writing - original draft. **Dian Zhong:** Formal analysis. **Gilles Flamant:** Supervision, Formal analysis, Writing - review & editing.

Declaration of competing interest

The authors declare that they have no known competing financial interests or personal relationships that could have appeared to influence the work reported in this paper.

Acknowledgement

This work was supported by French “Investments for the future” program managed by the National Agency for Research under contract ANR-10-LABX-22-01 (Labex SOLSTICE) and award number “ANR-10-EQPX-49-SOCRATE” (Equipex SOCRATE). Authors thank Eric Beche (PROMES-CNRS) for his assistant to Raman analysis.

Appendix A. Supplementary data

Supplementary data to this article can be found online at https://doi.org/10.1016/j.energy.2020.118128.

References

[1] Suzaki PYR, Munaro MT, Triques CC, Kleinübing SJ, Klen MRF, Jorge LMM, Bergamasco R. Biosorption of binary heavy metal systems: phenomenological mathematical modeling. Chem Eng J 2017;313:364–73.
[2] Liu WJ, Li WW, Jiang H, Yu HQ. Fates of chemical elements in biomass during its pyrolysis. Chem Rev 2017;117:6367–98.
[3] Said M, Cassayre L, Dirion J, Nzihou A, Joulia X. Influence of nickel on biomass pyro-gasification: coupled thermodynamic and experimental investigations. Ind Eng Chem Res 2018;57:9788–97.
[4] Yousaf B, Liu GJ, Abbas Q, Ali MU, Wang RW, Ahmed R, Wang CM, Al-Wabel MI, Usman ARA. Operational control on environmental safety of potentially toxic elements during thermal conversion of metal-accumulator invasive ragweed to biochar. J Clean Prod 2018;195:458–69.
[5] Chen T, Zhang YX, Wang HT, Lu WJ, Zhou ZY, Zhang YC, Ren LL. Influence of pyrolysis temperature on characteristics and heavy metal adsorptive performance of biochar derived from municipal sewage sludge. Bioresour Technol 2014;164:47–54.
[6] Zeng K, Li R, Pham Minh D, Weiss-Hortala E, Nzihou A, He X, Flamant G. Solar pyrolysis of heavy metal contaminated biomass for gas fuel production. Energy 2019;187:116016.
[7] Liu W, Tian K, Jiang H, Zhang X, Ding H, Yu H. Selectively improving the bio-oil quality by catalytic fast pyrolysis of heavy-metal-polluted biomass: take copper (Cu) as an example. Environ Sci Technol 2012;46:7849–56.
[8] Dilks RT, Monette F, Glaus M. The major parameters on biomass pyrolysis for hyperaccumulative plants – a review. Chemosphere 2016;146:385–95.
[9] Koppolu L, Clements LD. Pyrolysis as a technique for separating heavy metals from hyperaccumulators. Part I: preparation of synthetic hyperaccumulator biomass. Biomass Bioenergy 2003;24:69–79.
[10] Koppolu L, Agblevor FA, Clements LD. Pyrolysis as a technique for separating heavy metals from hyperaccumulators. Part II: lab-scale pyrolysis of synthetic hyperaccumulator biomass. Biomass Bioenergy 2003;25:651–63.
[11] Koppolu L, Prasad R, Clements LD. Pyrolysis as a technique for separating heavy metals from hyperaccumulators. Part III: pilot-scale pyrolysis of synthetic hyperaccumulator biomass. Biomass Bioenergy 2004;26:463–72.
[12] Zeng K, Gauthier G, Soria J, Mazza G, Flamant G. Solar pyrolysis of carbonaceous feedstocks: a review. Sol Energy 2017;156:73–92.
[13] Zeng K, Gauthier D, Li R, Flamant G. Solar pyrolysis of beech wood: effects of pyrolysis parameters on the product distribution and gas product composition. Energy 2015;93:1648–57.
[14] Zeng K, Gauthier D, Li R, Flamant G. Combined effects of initial water content and heating parameters on solar pyrolysis of beech wood. Energy 2017;125:552–61.
[15] Zeng K, Gauthier D, Pham Minh D, Weiss-Hortala E, Nzihou A, Flamant G. Characterization of solar fuels obtained from beech wood solar pyrolysis. Fuel 2017;188:285–93.
[16] Hervy M, Berhanu S, Weiss-Hortala E, Chesnaud A, Gérente C, Villot A, Pham Minh D, Thorel A, Coq LL, Nzihou A. Multi-scale characterisation of chars mineral species for tar cracking. Fuel 2017;189:88–97.
[17] Zeng K, Pham Minh D, Gauthier D, Weiss-Hortala E, Nzihou A, Flamant G. The effect of temperature and heating rate on char properties obtained from solar pyrolysis of beech wood. Bioresour Technol 2015;182:114–9.
[18] Guizani C, Haddad K, Limousy L, Jeguirim M. New insights on the structural evolution of biomass char upon pyrolysis as revealed by the Raman spectroscopy and elemental analysis. Carbon 2017;119:519–21.
[19] Li RH, Huang H, Wang JJ, Liang W, Gao PC, Zhang ZQ, Xiao R, Zhou BY, Zhang XF. Conversion of Cu(II)-polluted biomass into an environmentally

benign Cu nanoparticles-embedded biochar composite and its potential use on cyanobacteria inhibition. J Clean Prod 2019;216:25–32.
[20] Wang L, Li T, Güell BM, Løvås T, Sandquist J. An SEM-EDX study of forest residue chars produced at high temperatures and high heating rate. Energy Procedia 2015;75:226–31.
[21] He J, Strezov V, Kan T, Weldekidan H, Asumadu-Sarkodie S, Kumar R. Effect of temperature on heavy metal(loid) deportment during pyrolysis of Avicennia marina biomass obtained from phytoremediation. Bioresour Technol 2019;278:214–22.
[22] Keller C, Ludwig C, Davoli F, Wochele J. Thermal treatment of metal-enriched biomass produced from heavy metal phytoextraction. Environ Sci Technol 2005;39:3359–67.
[23] Davidsson KO, Stojkova BJ, Pettersson JBC. Alkali emission from birchwood particles during rapid pyrolysis. Energy Fuels 2002;16:1033–9.
[24] Kowalski T, Ludwig C, Wokaun A. Qualitative evaluation of alkali release during the pyrolysis of biomass. Energy Fuels 2007;21:3017–22.
[25] Nzihou A, Stanmore B, Lyczko N, Pham Minh D. The catalytic effect of inherent and adsorbed metals on the fast/flash pyrolysis of biomass: a review. Energy 2019;170:326–37.
[26] Liu Y, Guo F, Li X, Li T, Peng K, Guo C, Chang J. Catalytic effect of iron and nickel on gas formation from fast biomass pyrolysis in a microfluidized bed reactor: a kinetic study. Energy Fuels 2017;31:12278–87.
[27] Liu XH, Zheng Y, Liu ZH, Ding HR, Huang XH, Zheng CG. Study on the evolution of the char structure during hydrogasification process using Raman spectroscopy. Fuel 2015;157:97–106.
[28] Xu M, Hu HY, Yang YH, Huang YD, Xie K, Liu H, Li X, Yao H, Naruse I. A deep insight into carbon conversion during Zhundong coal molten salt gasification. Fuel 2018;220:890–7.
[29] Sheng CD. Char structure characterised by Raman spectroscopy and its correlations with combustion reactivity. Fuel 2007;86:2316–24.
[30] He X, Zeng K, Xie YP, Flamant G, Yang HP, Yang XY, Nzihou A, Zheng AQ, Ding Z, Chen HP. The effects of temperature and molten salt on solar pyrolysis of lignite. Energy 2019;181:407–16.
[31] Tay HL, Kajitani S, Wang S, Li CZ. A preliminary Raman spectroscopic perspective for the roles of catalysts during char gasification. Fuel 2014;121:165–72.
[32] Fu P, Hu S, Xiang J, Sun LS, Su S, Wang J. Evaluation of the porous structure development of chars from pyrolysis of rice straw: effects of pyrolysis temperature and heating rate. J Anal Appl Pyrol 2012;98:177–83.
[33] Lu LM, Kong CH, Sahajwalla V, Harris D. Char structural ordering during pyrolysis and combustion and its influence on char reactivity. Fuel 2002;81:1215–25.
[34] Stals M, Thijssen E, Vangronsveld J, Carleer R, Schreurs S, Yperman J. Flash pyrolysis of heavy metal contaminated biomass from phytoremediation: influence of temperature, entrained flow and wood/leaves blended pyrolysis on the behaviour of heavy metals. J Anal Appl Pyrol 2010;87:1–7.
[35] Shen YF, Chen MD, Sun TH, Jia JP. Catalytic reforming of pyrolysis tar over metallic nickel nanoparticles embedded in pyrochar. Fuel 2015;159:570–9.
[36] Azargohar R, Nanda S, Kozinski JA, Dalai AK, Sutarto R. Effects of temperature on the physicochemical characteristics of fast pyrolysis bio-chars derived from Canadian waste biomass. Fuel 2014;125:90–100.
[37] Wang SS, Gao G, Li TC, Ok YS, Shen CF, Xue SG. Biochar provides a safe and value-added solution for hyperaccumulating plant disposal: a case study of Phytolacca acinosa Roxb. (Phytolaccaceae). Chemosphere 2017;178:59–64.
[38] Dong J, Chi Y, Tang YJ, Ni MJ, Nzihou A, Weiss-Hortala E, Huang QX. Partitioning of heavy metals in municipal solid waste pyrolysis, gasification, and incineration. Energy Fuels 2015;29:7516–25.
[39] Bert V, Allemon J, Sajet P, Dieu S, Papins A, Collet S, Gaucher R, Chalot M, Michiels B, Raventos C. Torrefaction and pyrolysis of metal-enriched poplars from phytotechnologies: effect of temperature and biomass chlorine content on metal distribution in end-products and valorization options. Biomass Bioenergy 2017;96:1–11.
[40] Huang H, Yao W, Li R, Ali A, Du J, Guo D, Xiao R, Guo Z, Zhang Z, Awasthi MK. Effect of pyrolysis temperature on chemical form, behavior and environmental risk of Zn, Pb and Cd in biochar produced from phytoremediation residue. Bioresour Technol 2018;249:487–93.
[41] Šyc M, Pohořelý M, Jeremiáš M, Vosecký M, Kameníková P, Skoblia S, Svoboda K, Punčochář M. Behavior of heavy metals in steam fluidized bed gasification of contaminated biomass. Energy Fuels 2011;25:2284–91.
[42] Bunt JR, Waanders FB. Trace element behaviour in the Sasol–Lurgi MK IV FBDB gasifier. Part 2 – the semi-volatile elements: Cu, Mo, Ni and Zn. Fuel 2009;88:961–9.
[43] Jin JW, Li YN, Zhang JY, Wu SC, Cao YC, Liang P, Zhang J, Wong MH, Wang MY, Shan SD, Christie P. Influence of pyrolysis temperature on properties and environmental safety of heavy metals in biochars derived from municipal sewage sludge. J Hazard Mater 2016;320:417–26.
[44] Wornat MJ, Hurt RH, Yang NYC, Headley TJ. Structural and compositional transformations of biomass chars during combustion. Combust Flame 1995;100:131–43.
[45] Okuno T, Sonoyama N, Hayashi JI, Li CZ, Sathe C, Chiba T. Primary release of alkali and alkaline earth metallic species during the pyrolysis of pulverized biomass. Energy Fuels 2005;19:2164–71.
[46] Lu SY, Du YZ, Zhong DX, Zhao B, Li XD, Xu MX, Li Z, Luo YM, Yan JH, Wu LH. Comparison of trace element emissions from thermal treatments of heavy metal hyperaccumulators. Environ Sci Technol 2012;46:5025–31.
[47] Wang L, Sandquist J, Varhegyi G, Güell BM. CO_2 gasification of chars prepared from wood and forest residue: a kinetic study. Energy Fuels 2013;27:6098–107.